Journal of Radiation and Nuclear Applications
An International Journal

http://dx.doi.org/10.18576/jrna/090102

Studies ZnO Nanoparticles Using Nuclear Technique (DBES), SEM & EDX

H. Ibrahim, M. Abdel-Rahman and Emad A. Badawi[*]

Physics Department, Faculty of Science, 61519, Minia University, Minia, Egypt.

Received: 28 Oct. 2023, Revised: 12 Nov. 2023, Accepted: 22 Dec. 2023.
Published online: 1 Jan 2024.

Abstract: A comprehensive study of the effect of chelating agent on the microstructural properties, particle size, and elemental composition of ZnO nanoparticles (NPs) synthesized by citrate sol-gel method is presented. Crystal structure, crystallite size, lattice parameters and micro-strain, as well as defect and dislocation density of ZnO NPs are investigated using X-rays diffraction (XRD) and positron annihilation Doppler broadening energy spectroscopy (DBES). ZnO NPs size and elemental composition are studied using scanning electron microscopy (SEM) and energy dispersive X-ray analysis, respectively. Using Positron Annihilation Doppler broadening Energy Spectroscopy (DBES). ZnO NPs size and elemental composition are studied using scanning electron microscopy (SEM) and energy dispersive X-ray analysis (EDX), respectively. The correlation between microstructural properties and DBES line-shape parameters at different chelating agent concentrations is also examined and published. Crystallite plot using Popa rules model revealed that crystallites at intermediate chelating agent concentrations are more isotropic as shown below, with clear spherical symmetry around optimum nucleation conditions. Good agreement between SEM estimated ZnO NPs size and XRD calculated crystallite size is observed around optimum nucleation conditions as shown before. S-parameter and W-parameter as a function of citric acid concentrations also confirm the behavior of isotropic and anisotropic as shown by Popa rule model XRD and Doppler broadening parameters.
.

Keywords: ZnO Nanoparticles; Citrate Route Sol-gel Method; Crystallite Size; Defect and Dislocation Density; SEM and EDX.

1 Introduction

The effect of anhydrous citric acid has been studied thoroughly in the presented work to find the optimum conditions for ZnO (NPs) synthesis with the maximum purity and minimum size [3]. The effect of chelating agent on the crystal structure, the crystallite size, the lattice micro-strain, defects, and the dislocation density of ZnO (NPs) is studied utilizing X-rays diffraction (XRD) and Doppler broadening spectroscopy technique based on positron annihilation interaction. Microstructure characterization of synthesized ZnO NPs has been carried out using both Williamson-Hall [10] and Rietveld [11] methods. Crystallite size, micro-strain, and lattice parameters are also studied using anisotropic size-strain model (Popa rules model [3,12]).
Positron annihilation technique is a non-destructive powerful technique used for material characterization [1-2]. It is widely applied in the microstructure studies of metal alloys, semiconductors, and polymers. It gives advantageous information concerning the defects nature of ZnO NPs. DBES (Doppler broadening energy spectroscopy) of the electron–positron annihilation radiation is described with two different line-shape parameters (S-parameters and W-parameters) which are sensitive to microstructural changes. The correlation between microstructural properties and line-shape parameters of positron annihilation DBES at various anhydrous citric acid concentrations is investigated. In addition, ZnO NPs size and elemental composition are studied using energy dispersive X-ray (EDX) analysis and scanning electron microscopy (SEM), respectively.

2 Experimental Details

The used chemical reagents from analytical grade (Techno Pharma Chem). They were applied as received from the producer without extra refinement. Chemical reagents were dissolved with de-ionized water (50 ml) to prepare the aqueous solutions as needed. ZnO (NPs) preparation by citrate route method is achieved using 0.09 M of zinc

[*]Corresponding author e-mail: emad.badawi@mu.edu.eg

acetate dihydrate: $Zn(C_4H_6O_4)_2$. $2H_2O$ as zinc source mixed with different concentrations (0.025 M – 0.2 M) of anhydrous citric acid (H_3Cit or $C_6H_8O_7$) which serves as chelating agent. ZnO (NPs) Size and elemental composition were determined utilizing JEOL SEM (JSM – IT 200) at 25 kV voltage of operation.

DBES technique is utilized to evaluate the samples of ZnO at the Positron Science Laboratory. DBES spectra were measured with approximately 2500 cps counting rate utilizing detector of HPGe (Ortec type with efficiency of 35% and 1.5 keV resolution at an annihilation peak of 511 keV). Samples spectra of DBES were taken at room temperature, after being pressed into pellets. Each sample spectrum saved with total counts of 2.0 million.

The DBES spectra of samples were characterized into two line-shape parameters (S and W). The S-parameter is the integrated counts area A relative to the total counts (**see Fig. 1**). The used wings energy ranges are 508.0 to 509.4 keV (left W width) and 512.6 to 514.0 keV (right W width). The definition of S- and W-parameters from Doppler broadening is shown schematically in **Fig. 1(a,b)**.

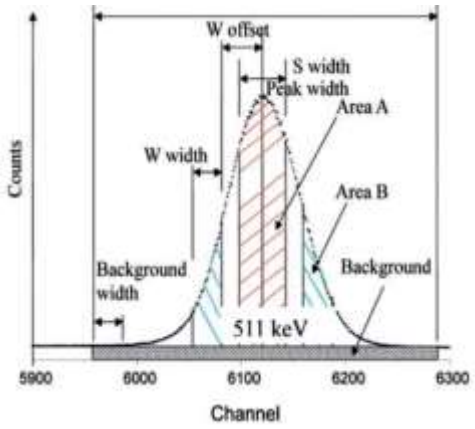

Fig. 1(a) DBES line shape S & W parameter [4]

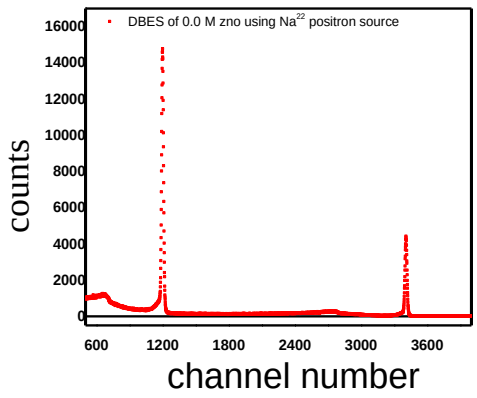

Fig.1 (b) DBES for ZnO nanoparticles synthesized. 0.0 M using Na^{22} positron source.

3 Results and Discussion

The obtained DBES spectra of the electron – positron annihilation radiation is analyzed using the SP program [4]. It is important to note that S-parameter is sensitive to annihilation with low momentum electrons. Positron annihilation with low momentum electrons takes place more frequently when defects concentration increases. As a result, more defects such as vacancies or voids in the material will cause an increase in the integrated counts between energy 510.3 and 511.7 keV (area A of **Fig. 1(a)**, which in turn will increase the value of S-parameter. **Fig. 1(b)** shows the spectrum for ZnO at 0.0 M using Na^{22} positron source. **Fig. 2 (a)** shows the evaluated line-shape S- and W-parameters at different citric acid concentrations. As shown, S-parameter initially increases with increasing citric acid concentration and then, at higher citric acid concentrations, starts to decrease. W-parameter which characterizes the positron annihilation with the high momentum electrons (annihilation with core electrons), however, has the reverse behavior of the S-parameter.

It is interesting to note that the behavior of the S-parameter as a function of citric acid concentration is almost opposite to that of ZnO crystallite size (**Fig. 2 a,b,c**). To further verify this, the S-parameter is plotted versus the crystallite size (**Fig. 2**). The obtained results agree well with the findings of Dutta *et al.* This is maybe due to the fact that decreasing crystallite size results in an increase in highly defective grain boundary regions, which in turn, will increase the value of S-parameter. To identify the nature of the positron trapping sites (defects); the S-parameter is plotted versus W-parameter (**Fig. 2**)a,b,c. Therefore, in ZnO, positrons tend to annihilate more at Zn vacancies rather than oxygen vacancies. Considering this fact as well as the findings of **Fig. 2(a,b,c)** we believe that Zn vacancies are the major type of defects existing in our samples. ZnO Synthesized at different parameter
concentrations of citric acid.

SEM images **Fig. 3(a)**, analyzed using ImageJ bundled with Java program used to estimate the average ZnO NPs size. The particle size distribution estimated from the SEM images analyzed by the ImageJ program. The average nanoparticle size has been determined from the histogram. Also, we have found that, as a function of citric acid concentration, particle size behaviors in the same manner as nano-crystallite size. **Fig. 3(a)** shows SEM images for ZnO samples synthesized at citric acid concentration of 0.025 M. The inset of **Fig. 3(a)** represents the particle size distribution estimated from the SEM images analyzed by the ImageJ program. The average nanoparticle size has been determined from the histogram. We have found out that, as a function of citric acid concentration, particle size behaves in the same manner as nano-crystallite size.

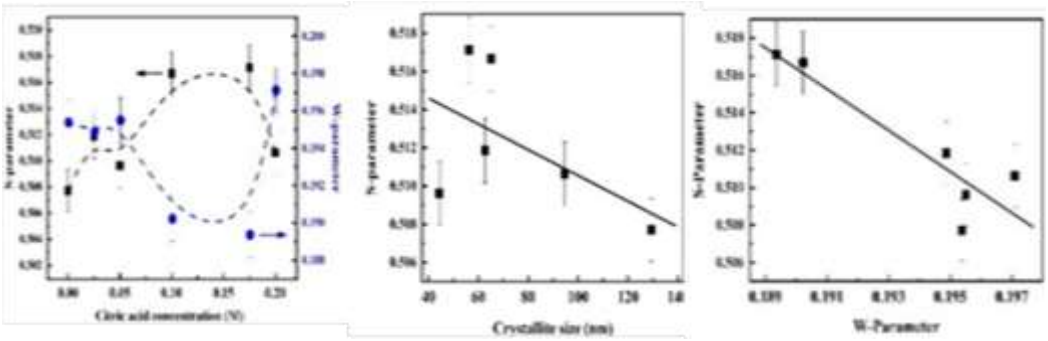

Fig. 2 (a) Line-shape S- and W-Parameters of nanoparticle concentrations of citric acid.

Fig. 2 (b) S-parameter as a function of Crystallite size nm.

Fig. 2(c) S parameter as a f unction of W parameter Synthesized at different .

Good agreement between estimated particle size and XRD calculated crystallite size is observed [3] only around optimum nucleation conditions (small crystallite size). At citric acid concentration of 0.025 M (**Fig. 3(a)**), the average particle size (66.84 nm) agrees well with the nano crystallite size calculated by 3 different techniques [3]. In the meantime, away from such optimum conditions (at high citric acid concentration, > 0.1 M), significant differences are observed between estimated particle size and calculated crystallite size. At citric acid concentration of 0.2 M, for instance, the average particle size (222.66 nm) is much larger than the crystallite size calculated from the XRD analysis [3-5]. We believe that the slow nucleation process due to the lack of zinc citrate complex formation that takes place at high citric acid concentration is responsible for particles agglomeration which is the reason for the observed difference. It is worth noting that other researchers have previously reported differences between SEM/TEM estimated particle size and XRD calculated crystallite size in nanocrystal line ZnO synthesized via sol-gel [7-9] and other chemical route methods. Our results corroborate that XRD calculated crystallite size does not necessarily match the real nanoparticle size and should not be used solely to estimate the nanoparticle size. From the above results using different methods of XRD Williamson-Hall method, Rietveld method and Popa rules model with SEM it is clear the concentration of citric acid from 0.025 to 0.175 M have lower minimum 44.4 nm size to the maximum values of size about 70.88 nm. It is also we can realize that the optimum concentration of citric acid varies from 0.025 to 0.175 M as isotropic. EDX spectroscopy of ZnO NPs [6] synthesized at citric acid concentration of 0.025 M is shown in **Fig. 3(a,b)** In addition to zinc and oxygen, traces of carbon are detected as indicated by the small impurity peak observed near the origin at ~ 0.28 keV. **It is clear** Crystallite plot using Popa rules model for nanoparticles of ZnO synthesized at different concentrations of citric acid as shown below.

Lattice parameters, micro-strain, and crystallite size determined by analyzing XRD patterns using Rietveld software: Materials Analysis Using Diffraction (MAUD) program [1].

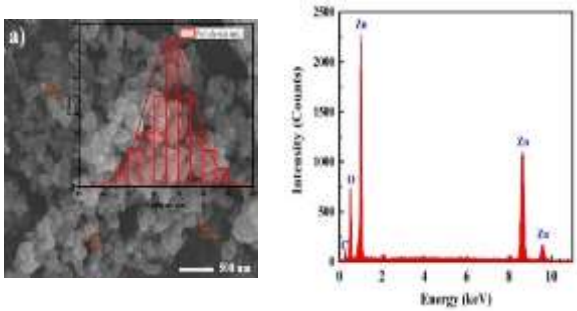

Fig. 3 (a,b). SEM images(a) and EDX (b)spectroscopy of nanoparticles ZnO Synthesized at 0.025 M citric acid.

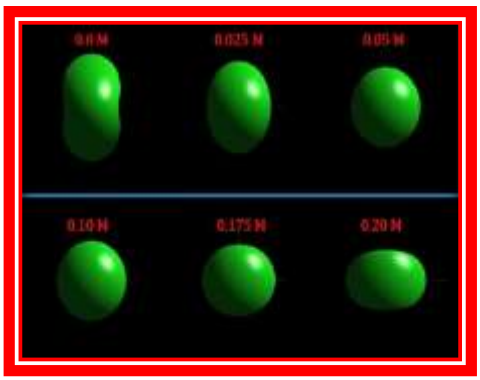

Fig. 4. Crystallite plot using Popa rules model for nanoparticles of ZnO synthesized at different concentrations of citric acid.

4 Conclusions

From the results we can conclude that the optimum concentration of citric acid gives reliable values of crystallites size and micro stain analyses by three XRD method. At low concertation of citric acid 0.0 M and high

concertation of citric acid above 0.1 M crystallites at very low and very high anhydrous citric acid concentrations are completely anisotropic. Obtain the optimum conditions for ZnO NPs. At (< 0.025 M), citric acid is not sufficient to completely reaction.

Optimum nucleation 0.025 M – 0.175 M of anhydrous citric acid, with smallest particle size of 44.4 nm obtained at 0.05 M concentration. Good agreement between SEM, DBES calculated crystallite size and others. S-parameter and W-parameter as a function of citric acid concentrations also confirm the behavior of isotropic and anisotropic by Popa rule model XRD and DBES.

Acknowledgement

Authors wish to express appreciation Prof. Dr. Mamdouh Abdel Nasser, Professor of Exp. Nuclear Physics, faculty of Science, Minia University, for his helpless, effort and interesting discussion. Also, We Wish to express our deepest appreciation **to the Soul of** Dr. M. Rafit Ebid. For his suggest research point and valuable discussion.

References

[1] Sayed, Z., Abdel-Rahman, M. Mostafa, M. Y. A., Abdel-Rahman, M. A., Badawi, E. A., Assem, E. E., Ashour, A. Structural of the deformed 7075 aircraft Al alloy with material analysis using diffraction (MAUD). Int. J. thin film. Sci. Tec. 11, No. 3. 267-274 (2022).

[2] Abdel-Rahman, M., Ibrahim, H., Mostafa, M. Y. A., Abdel-Rahman, M. A., Ebied, M. R. and Badawi, E. A. The characterization of ZnO nanoparticles by applying x-ray diffraction and different methods of peak profile analysis Physica Scripta 96 095704 (2021).

[3] R. Janisch, P. Gopal, and N. Spaldin, Transition metal-doped TiO2 and ZnO – present status of the field, J. Phys. Condens. Matter. 17 (2005) R657-R689

[4] Abd-Elhakim, M. H., Mostafa, Y. A. M., Darwash, M., Abdel-Rahman, M., Abdel-Rahman, M. A. and Badawi E. A. Probing properties of 6061 aluminum alloy used as cladding for nuclear reactor fuel with X-ray diffraction. AIP Conference Proceedings 2313, 060021 (2020).

[5] Ouyang W, Chen J, Shi Z and Fang X Self-powered UV photodetectors based on ZnO nanomaterials Applied Physics Reviews 8, 031315 1-28 (2021).

[6] Khan, A. R., Azhar, W., Wu, J., Ulhassan, Z., Salam A, Zaidi S H R, Yang S, Song G and Gan, Y. Ethylene participates in zinc oxide nanoparticles induced biochemical, molecular and ultrastructural changes in rice seedlings Ecotoxicology and Environmental Safety 226 112844 (2021).

[7] Khatami, M., Varma R. S., Zafarnia, N., Yaghoobi. H., Sarani, M., Kumar, V. G. Applications of green synthesized Ag, ZnO and Ag/ZnO nanoparticles for making clinical antimicrobial wound-healing bandages Sustainable Chemistry and Pharmacy 10 9–15 (2018).

[8] Rad, S. S., Sani, A. M., Mohseni, S. Biosynthesis, characterization and antimicrobial activities of zinc oxide nanoparticles from leaf extract of Mentha pulegium (L.) Microbial Pathogenesis 131 239-45 (2019).

[9] Ginjupalli, K., Alla, R., Shaw, T., Tellapragada, C., Kumar, G. L., Nagaraja, U. P. Comparative evaluation of efficacy of Zinc oxide and Copper oxide nanoparticles as antimicrobial additives in alginate impression materials Materials Today: Proceedings 5 16258–66 (2018).

[10] G. Williamson, W. Hall, X-ray line broadening from filed aluminium and wolfram, Acta Mettal. 1 (1953) 22 – 31. https://doi.org/10.1016/0001-6160(53)90006-6

[11] H. Rietveld, A Profile Refinement Method for Nuclear and Magnetic Structures, J. Appl. Cryst. 2 (1969) 65 – 71. https://doi.org/10.1107/S0021889869006558

[12] N. Popa, The (HYPERLINK "https://journals.iucr.org/j/issues/1998/02/00/th0009/th0009.pdf"hkl HYPERLINK "https://journals.iucr.org/j/issues/1998/02/00/th0009/th0009.pdf") Dependence of Diffraction-Line Broadening Caused by Strain and Size for all Laue Groups in Rietveld Refinement, J. Appl. Cryst. 31 (1998) 176 – 180. https://doi.org/10.1107/S0021889897009795